Coupling SiNAPS High-density Neural Recording CMOS-Probes with Optogenetic Light Stimulation

Fabio Boi*, Andrea Locarno†, Joao F. Ribeiro*, Raffaella Tonini†, Gian Nicola Angotzi* and Luca Berdondini*
Email: {fabio.boi, andrea.locarno, joao.ribeiro, raffaella.tonini, giannicola.angotzi, luca.berdondini}@iit.it
*Microtechnology for Neuroelectronics, Fondazione Istituto Italiano di Tecnologia, Genova, Italy.
†Neuromodulation of Cortical and Subcortical Circuits, Fondazione Istituto Italiano di Tecnologia, Genova, Italy.

2021 IEEE Biomedical Circuits and Systems Conference (BioCAS) | 978-1-7281-7204-0/21/$31.00 ©2021 IEEE | DOI: 10.1109/BIOCAS49922.2021.9645041

***Abstract* - Optogenetic light stimulation is a key neuromodulation technology for the study of brain circuits in animal models. A powerful approach to advance the recording of such light-evoked responses consists in coupling this technology with new generations of CMOS-based implantable neural probes that can provide sub-millisecond recordings from thousands of closely spaced electrodes. Among CMOS-probes, SiNAPS probes are the only ones that use small-area DC-coupled electrode-pixel and on-probe read-out circuits to simultaneously record full-bandwidth neural signals from all integrated electrodes. Here, we experimentally investigate the performances of 4-shank SiNAPS probes with 1024 electrodes to record light-evoked responses from wide brain areas in mice. Light stimuli were delivered from an implanted optical fiber placed at <1 mm distance from the closest recording site. Proof-of-concept results show *in vivo* recordings of optogenetic responses, both action potentials (APs) and low-frequency field potentials (LFPs), and demonstrate the performances of SiNAPS probes to simultaneously acquire evoked activity across multiple brain circuits and wide brain area.**

I. INTRODUCTION

The ability to selectively perturb and record hundreds to thousands of neurons across large brain circuits can provide the technological ground for innovative experimental tools to study in animal models brain circuits under health and diseased conditions [1]. Although optogenetics is nowadays a widely used technique to study brain circuits by selectively controlling the activity of neurons expressing light-modulated opsins [2], [3], conventional electrode technologies for sub-millisecond recordings of light-evoked activities are typically limited to a few tens of neurons.

With respect to conventional Si-probes realized by MEMs processes, the recent introduction of implantable active neural probes based on microstructured monolithic complementary metal-oxide semiconductor (CMOS) devices (i.e. Neuropixels [4], [5], NeuroSeeker [6] and SiNAPS [7], [8]) allows to considerably scale up the number of recorded neurons within and across multiple brain circuits [9]. For instance, recent studies have demonstrated the possibility of combining Neuropixels recordings with optogenetic stimulation of both excitatory and inhibitory neural populations *in vivo* [4], [5].

Among the proposed CMOS-probe circuits, CMOS-based SiNAPS probes are built on a radically different circuit architecture, which uniquely enables the unrestricted simultaneous recording from all integrated electrodes. The circuitry of these probes consists of modules of 32 electrode-pixels which makes the SiNAPS technology highly modular, thus ideal for the rapid design of different probe layouts. Initially demonstrated with a 512 electrode single-shank probe layout [7], we recently presented (Fig. 1) a 4-shank version with 1024 electrodes (electrode pitch of 28 µm) that was realized in standard 180 nm CMOS technology by "copy and paste" the basic circuit modules [8]. Rather than integrating front-end amplifiers on the base of the probe as in Neuropixels or NeuroSeeker devices, our SiNAPS probes integrate DC-coupled front-ends underneath each single electrode. This *one-to-one* correspondence between electrodes and amplifiers allows reaching the objective of continuously recording at sub-millisecond resolution from all the integrated electrodes, as well as to define an architecture that simplifies the realization of probes with different layouts and number of recording sites.

These probes were not yet demonstrated to record neural activity responses upon optogenetic light stimulation. Here, we discuss results obtained by combining optogenetics with electrical recordings using a 4-shank SiNAPS probe with 1024 simultaneously recording electrodes. Specifically, our preliminary recordings report light-evoked neural activity in

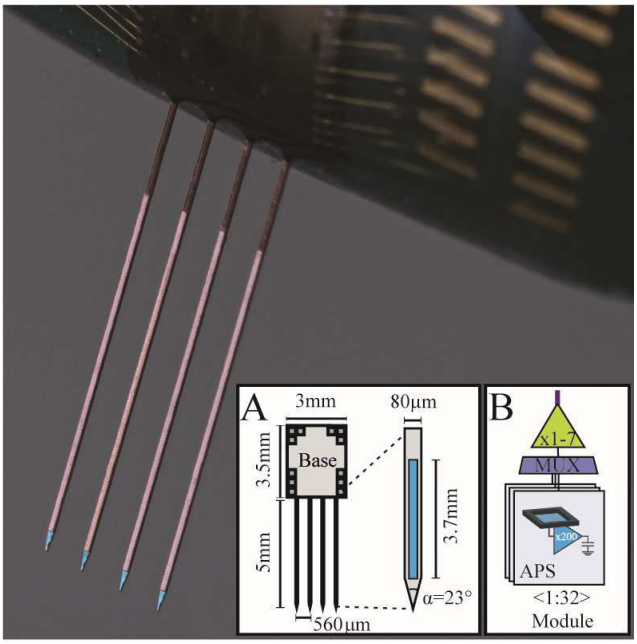

Fig. 1: Overview of a four shanks SiNAPS probe mounted on a PCB. Inset in Panel A reports probe dimensions, with the active area (in blue) of each shank obtained by replicating 8 times a 32 electrode-pixel module whose schematic architecture is shown in panel B.

the cortex and striatum and, most importantly, confirm the possibility of exploiting SiNAPS probes for investigating optogenetic response dynamics both at the single-neuron and large-scale network level with high spatiotemporal resolution and from wide brain areas.

II. Materials and Methods

A. System Architecture

A complete system was designed for controlling the SiNAPS probe operation and for data acquisition. More in detail, the data acquisition signal chain consists of a SiNAPS probe that provides low-noise neural signal amplification (46dB gain, 0-4kHz signal bandwidth) for the whole array of 1024 electrode-pixels that are time division multiplexed to only 32 output pads. A bank of 32 analog to digital converters (MAX11105 – Maxim Integrated, USA) is used for 12-bit digitalization of the analog traces produced by the SiNAPS probe, with a sampling rate of 20kSample/electrode-pixel. A Digital Control unit (DCU) was implemented on the ZEM4310 integration module based on the Altera Cyclone IV FPGA. It provides the digital control signal required for correct operations of the SiNAPS probe (device initialization, and time division multiplexing operation), controls operation and data readout for the bank of ADCs, implements a camera link protocol for real-time data transfer (~250Mbps) to a PC and, finally, provides time synchronization with the external laser used for optogenetic stimulations. Finally, an adapted release of the BrainWave data acquisition software (3Brain AG– Switzerland) was used for data visualization and storage on a PC.

B. CMOS post-processing

CMOS single dies are delivered with 3 mm width, 8.5 mm length and 250 µm thickness. Since the native Aluminum/Copper alloy (Al/Cu) CMOS metallization of the electrodes (15×15 μm^2 apertures on the surface passivation layer) is not a suitable electrode material, a dual photoresist layer lift-off process is used to pattern Platinum (Pt) electrodes on top of the Al/Cu layer. First, the dies are fastened with a water dissoluble glue in a glass slide to handle them during processing. Then a layer of LOR 3B followed by a layer of S1813 photoresist are deposited and patterned to archive electrodes with 19×19 μm^2 ensuring the full coverage of the Al/Cu layer and the side walls of the CMOS encapsulation layer. We deposited a 10 nm thick Titanium (Ti) layer on top of the Al/Cu CMOS layer, and a 100 nm thick Pt layer using the electron beam technique at 0.4 Å/s. After the metal deposition, remover PG is used to remove the photoresist layers. To guarantee the stability of the recordings, a conformal 25 nm silicon oxide (SiO_2) layer is deposited at 80 °C by Atomic Layer Deposition (ALD) on the backside and sides of the device. Structured probes were finally mounted to small printed circuit boards (PCB), with the IO pad area encapsulated with Ostemer resin to protect wire bonds.

C. Experimental procedure

C57BL/6J mice (4-6 weeks old) were anesthetized with a O_2 isoflurane (1-1.5%) mix and placed on a stereotaxic frame. 0.5µl per hemisphere (~10^{13} genome copies/ml) of a viral construct bearing ChR2 (AAV5-CaMKIIα-hChR2(H134R)-EYFP, Addgene) was injected into the Prefrontal Cortex (PFC, from bregma: AP +1.25, ML +0,4, DV-1.4) at a rate of 0.1 µl/min. 4-6 weeks after surgery mice underwent electrophysiology experiments. Animals were anesthetized (induction 4% isoflurane/O_2 mix, maintenance 1-1.5% isoflurane/O_2 mix) and placed on a stereotaxic frame. As illustrated in Fig. 2, a craniotomy was performed at the stereotaxic coordinates for optic fiber implantation (from bregma: AP +2.6, ML +0.4) and an optic fiber (200µm, 0.39NA, RWD) was lowered into the PFC (-2.0mm, 45° anteroposterior angle). A larger cranial window (2.5mm x 2.5mm) was drilled centered at the site of the probe insertion (from bregma: AP +0.94, ML +1.72) and a 4-shank SiNAPS probe was lowered into the brain (from brain surface: DV -4.5). The relative estimated anteroposterior gap between the optic-fiber tip and the closest probe electrode was ~0.5 mm. For optogenetic stimulation, a laser source (Laserglow Technologies) was used to deliver 50 blue light pulses (10ms, 473nm) at 5mW power at the fiber tip.

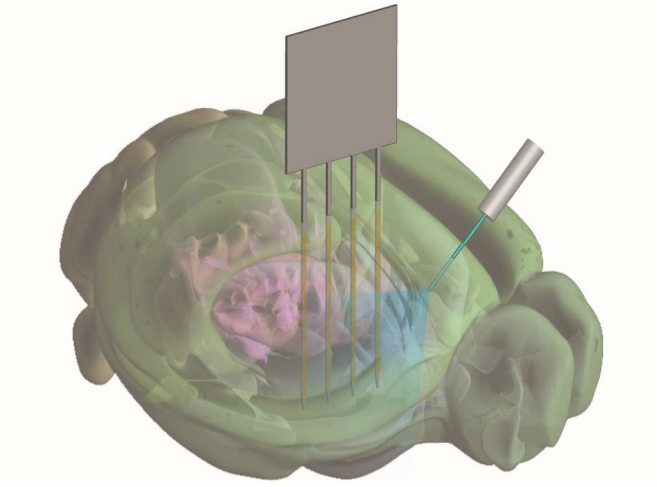

Fig. 2: Schematic 3D view of the experimental condition. The SiNAPS probe and the optic fiber are superimposed to a 3D model of a mouse brain in order to illustrate their relative position.

D. Histology

After electrophysiology experiments, the location of the optic fiber tip was verified by histology. Mice were perfused with 4% paraformaldehyde (w/v) in phosphate buffer (0.1M PB; pH 7.4) and microtome sections (20 µm) were obtained. Sections were then washed three times in PB solution and the cell nuclei were stained with DAPI. Brain slices were mounted on glass slides, and coverslipped with ProLong Gold antifade reagent (ThermoFisher Scientific, Carlsbad, California). 5x confocal images of the fiber optic-tip trace were acquired with an inverted Leica SP5 confocal microscope (dashed red circle, Fig. 3).

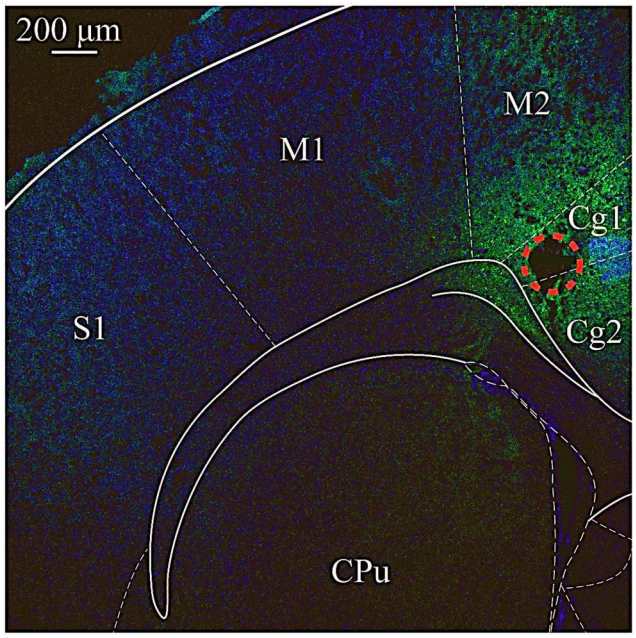

Fig. 3 Example confocal image showing the expression of the AAV5-CaMKIIα-hChR2(H134R)-EYFP in the cortex and the position of the optic fiber trace (red dashed circle) (green GFP, blue DAPI).

E. Data analysis

Broadband data acquired during the experimental sessions were post-processed off-line using *band-pass FIR filter*s implemented on Matlab, with cut-off frequencies defined as follows:

1) Spike sorting

Raw neural signals were band passed filtered in the 300 Hz-5 kHz frequency band. To isolate single units, the resulting neural traces were processed using the Kilosort 2 [10] spike sorting software whose output was ultimately refined by manual curation using the Phy graphical user interface.

2) Low-frequency evoked activity map

To generate the low-frequency evoked activity maps of LFP discussed in section III.B, neural signals were first filtered in the 1-300 Hz frequency band. Then, across a total of 50 trials and for all the 1024 available recording sites, we averaged the first 50 ms time window following the onset of each light stimulus and computed the peak-to-peak amplitude of the resulting waveforms. Finally, to obtain false-color maps describing the low-frequency evoked activity we interpolated such peak-to-peak values in a bi-dimensional plane (using *Griddata* Matlab function, *natural* method).

III. Results and Discussion

To assess the possibility of combined SiNAPS recordings and optogenetic stimulation we performed experimental sessions in head-fixed anesthetized mice expressing ChR2 in principal cortical neurons. We achieved selective expression of ChR2 in these neurons by using a Ca2+/calmodulin-dependent protein kinase II α (CamKIIα) promoter [11], [12]. We aimed at recording the connectivity between two different brain regions (cortex and striatum) with a high spatiotemporal resolution in order to identify the range of neural activity dynamics upon optogenetic activation. The architecture of our probe allowed us to simultaneously record light-evoked LFPs and APs neural activities from a large portion of the cortex and striatum, without compromising single-cell resolution.

A. Single units light-evoked responses

During a single experiment, we recorded the electrical activity of more than 150 well isolated neuronal cells spread across different cortical and striatal circuits over almost 7 mm^2 (see Fig. 4A). As shown, single-unit recordings are characterized by a wide variety of spiking activity dynamics in response to light stimuli. As reported in Fig. 4B, both close and distant (various millimeters away from the tip of the optic fiber) neurons show a peaked response induced by the optogenetic light pulse. Interestingly, we did not observe a direct correlation between the strength and the speed of the evoked spiking activity (in terms of firing rate and time-delay) with respect to the relative distance between the recorded neurons and the fiber optic tip. This may suggest an indirect activation of these cells through their underlying neural circuits. The relative position between the optic fiber and our probe allowed us to record neural activity propagating across synaptically connected regions such as the PFC and the dorsal and ventral parts of the striatum.

B. Low-Frequency light-evoked responses

We subsequently analyzed the effects of optogenetic stimulation on the low-frequency components (1-300 Hz) of the neural signal. The Fig 5B shows some representative broad-band traces recorded from five neighboring channels simultaneously collected from each shank of the probe. As

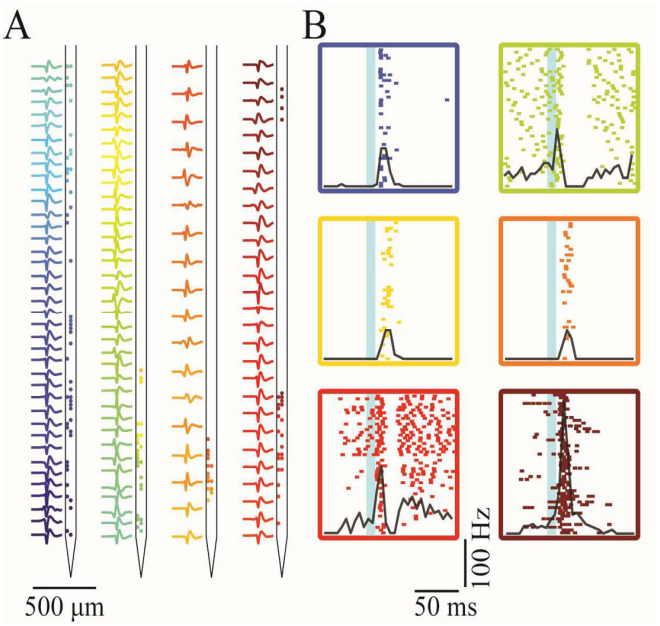

Fig. 4 Single-unit light-evoked responses. (A) 4-shank probe representation with spike waveforms of the isolated single unit responses. Colored dots on the shanks represent the location of single units on the probe. (B) Examples of the spike rasters and peri-stimulus histograms upon optogenetic stimulation of 6 isolated single units. Color-code represents the relative position of the isolated single-units on the probe. Light-blue rectangles represent the period in which the optostimulation is on.

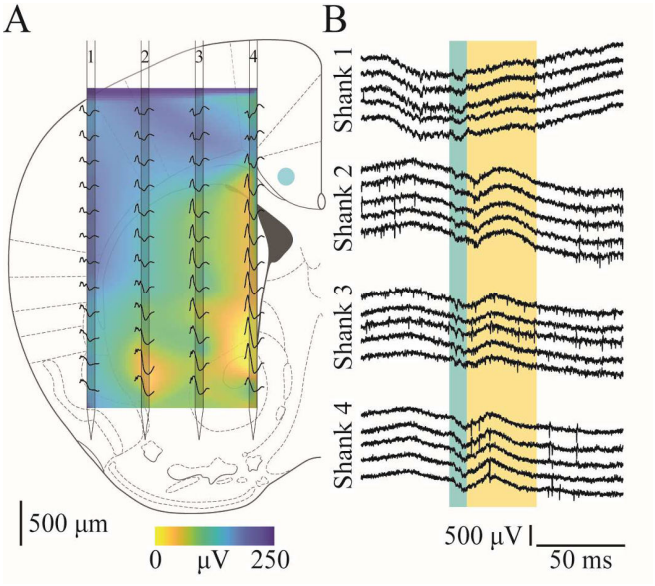

Fig. 5 Optogenetic LFP light-evoked responses. (A) 4-shank probe position during experiment superimposed to the approximate mouse atlas coronal section (Allen Mouse Brain Atlas). Black curves report some representative portion (50 ms) of the LFP responses collected along the probe shanks after the light stimulus onset. False-color map represents the interpolated peak-to-peak values of the low frequency responses over the probe bidimensional plane. Blue circle highlights the estimated fiber tip position projected on the probe coronal plane. (B) Example of the broadband signals recorded from 5 neighboring channels sampled from the 4 different shanks. Blue rectangle represents light stimulation, yellow rectangle shows the time used to generate the false-color map.

described in section II.A.2), for each electrode we considered only the 50ms LFP signal following the onset of each light-stimulus. The resulting waveforms (a representative subset is depicted in Fig. 5A) once placed in correspondence of the belonging electrode location clearly show the spatial evolution of the LFP light-evoked responses over the observed brain area. To better represent this gradient,we computed the peak-to-peak amplitudes of the LFP waveforms by interpolating them over the probe bi-dimensional plane; we obtained a false-color map that undoubtedly shows the spatial relationship between the fiber tip location (blue circle in Fig 5A) and the light-evoked low-frequency neural activity over the brain tissue.

IV. Conclusion

This work firstly demonstrates the possibility of combining SiNAPS probes with short distance (<1mm) optogenetic stimulation for high-resolution electrical recordings of light-evoked neural activity *in-vivo*. Specifically, our preliminary results suggest two opposite behaviors of neural activity in response to opto-stimulation: while the low-frequency activity seems to follow a predictable gradient that proportionally decays with the increase of the relative distance between the recording sites and the optic fiber, the single units evoked activity is more unpredictable, since it is determined by the underlying brain circuit that allows synaptic communication between light-activated neurons at the cortical stimulation site and neurons at the recording sites.

The brain operates with large-scale neural networks that spread over different brain areas, and ultimately to the entire brain. In this respect, these results reveal the importance of developing recording technologies able to sample with high spatiotemporal resolution contiguous and localized brain areas, but also to simultaneously record evoked responses from wide portions of the cerebral tissue. In this framework, SiNAPS probes represent the only currently available CMOS-based devices that can simultaneously access evoked neuronal activity from different and sparse brain circuits at high spatiotemporal resolution. Ultimately, the just proven possibility to couple our technology with standard optogenetic tools paves the way to the design of new experimental studies to gain a better understanding of the implementation and execution of distributed brain functions in health and disease.

Acknowledgment

This work was supported by IIT – NetS^3 lab and by ChroMOS project H2020-MSCA-IF-2019 grant agreement 896996. The authors also thank the IIT technicians and clean-room staff for technical support.

References

[1] J. P. Seymour, F. Wu, K. D. Wise, and E. Yoon, "State-of-the-art mems and microsystem tools for brain research," *Microsystems Nanoeng.*, vol. 3, no. July 2016, pp. 1–16, 2017.

[2] P. Rajasethupathy, E. Ferenczi, and K. Deisseroth, "Targeting Neural Circuits," *Cell*, vol. 165, no. 3, pp. 524–534, 2016.

[3] M. E. Carter and L. de Lecea, "Optogenetic investigation of neural circuits in vivo," *Trends Mol. Med.*, vol. 17, no. 4, pp. 197–206, 2011.

[4] N. A. Steinmetz *et al.*, "Neuropixels 2.0: A miniaturized high-density probe for stable, long-term brain recordings," *Science (80-.).*, vol. 372, no. 6539, 2021.

[5] J. J. Jun *et al.*, "Fully integrated silicon probes for high-density recording of neural activity," *Nature*, vol. 551, no. 7679, pp. 232–236, 2017.

[6] B. C. Raducanu *et al.*, "Time multiplexed active neural probe with 1356 parallel recording sites," *Sensors (Switzerland)*, vol. 17, no. 10, pp. 1–20, 2017.

[7] G. N. Angotzi *et al.*, "SiNAPS: An implantable active pixel sensor CMOS-probe for simultaneous large-scale neural recordings," *Biosens. Bioelectron.*, vol. 126, no. September 2018, pp. 355–364, 2019.

[8] F. Boi *et al.*, "Multi-shanks SiNAPS Active Pixel Sensor CMOS probe: 1024 simultaneously recording channels for high-density intracortical brain mapping," *bioRxiv*, p. 749911, 2019.

[9] A. Nurmikko, "Challenges for Large-Scale Cortical Interfaces," *Neuron*, vol. 108, no. 2, pp. 259–269, 2020.

[10] M. Pachitariu, N. Steinmetz, S. Kadir, M. Carandini, and K. Harris, "Fast and accurate spike sorting of high-channel count probes with KiloSort," in *Advances in Neural Information Processing Systems*, 2016.

[11] J. H. Lee *et al.*, "Global and local fMRI signals driven by neurons defined optogenetically by type and wiring," *Nature*, vol. 465, no. 7299, pp. 788–792, 2010.

[12] T. Dittgen *et al.*, "Lentivirus-based genetic manipulations of cortical neurons and their optical and electrophysiological monitoring in vivo," *Proc. Natl. Acad. Sci. U. S. A.*, vol. 101, no. 52, pp. 18206–18211, 2004.